Age of Information for Preemptive/Non-preemptive Transmissions in Large-Scale IoT Networks

Badiaa Gabr*, Hesham ElSawy⋆, Karim G. Seddik†, Wessam Mesbah‡
*New Giza University, Giza 12256, Egypt
⋆Queen's University, Kingston, Ontario, K7L 3N9 Canada
†American University in Cairo, New Cairo 11835, Egypt
‡King Fahd University of Petroleum and Minerals (KFUPM), Dhahran 31261, KSA

***Abstract*—In the Internet of Things (IoT) era, data freshness is critical for real-time monitoring and control applications. Data freshness is quantified via the Age of Information (AoI), which tracks the age of the most recent received packet at the destination. This paper utilizes a spatiotemporal mathematical model to characterize the AoI of a target IoT link that exists within a large-scale IoT network. The large-scale IoT network is modeled by a heterogeneous Poisson field (HPF) of interferers. Then, the AoI of the target link, with a single packet storage capability, is characterized via an absorbing Markov chain that accounts for the interwoven effects of packet size, transmission rate, and interfering IoT devices. In particular, the proposed model investigates the impact of packet segmentation in order to operate at a reliable rate in the presence of IoT interference. To this end, the AoI of preemptive and non-preemptive transmission schemes are studied and compared. Comparing the AoIs of the preemptive and non-preemptive transmission schemes, the results show that no scheme always outperforms the other. In contrast, the number of segments and preemption scheme should be determined based on the packet size, arrival rate, and interference congestion level to minimize the AoI.**

***keywords*—** Age of Information (AoI), Stochastic Geometry, Preemptive and Non-preemptive Queue.

I. Introduction

The proliferation of the Internet of Things (IoT) enables diverse devices, such as vehicles, home appliances, sensors, etc., to have ubiquitous Internet connectivity. The collective transmissions to monitor, control, and communicate with these IoT devices are foreseen to significantly overload current networks. In the context of time-critical IoT applications, lower latency is also required. Data freshness is evolving in monitoring and control applications as an important quality of service (QoS) parameter. The freshness of data means that a destination node (e.g., cloud or fog computing facility) should acquire an *always updated* version of the data collected by other IoT devices. Data freshness is measured through the Age of Information (AoI), which tracks the age of the latest received update at a destination node.

The AoI metric was first proposed to characterize the freshness of the received information in [1], [2]. For IoT applications, the AoI analysis needs to be extended for large-scale network setups with a massive number of devices. In this context, the authors in [3] proposed a three-phase transmission scheme that aggregates the data from multiple source-destination (SD) pairs into a mega update. It was shown that such aggregated data transmission could minimize the average AoI of each node. In [4] the authors discussed the optimal freshness transmission policy to guarantee a target age of received data. Based on time-variant interference constraints and channel state, the authors of [5] proposed virtual-queue-based and age-based policies to minimize AoI; they proved that the virtual-queue-based policy is closer to optimality than the age-based policy. Authors in [3]–[5] neither considered the spatial locations of SD pairs nor the mutual interference among different transmitters when analyzing the AoI. While authors in [6] considered the mutual interference among different nodes by focusing on the mobility of SD pairs and how it can affect the peak AoI (PAoI) in IoT networks. The authors introduced an iterative algorithm to minimize PAoI for mobile SD pairs by jointly optimizing energy and service time.

Under the assumption that users are spatially located according to a Poisson point process (PPP), a tractable mathematical model was introduced in [7] to characterize the spatiotemporal interactions by considering two different traffic models, where robust network connections can be guaranteed by power control at each user to mitigate the interference within the network. Therefore, spatial and temporal variations of users have to be considered due to their great impact on network stability. The authors of [8] investigated the PAoI within large-scale networks with un-segmented packets under the preemptive and non-preemptive schemes. In this paper, we employ the spatiotemporal distributions of SD pairs and their activities to calculate the mutual interference among different transmitters within a large-scale IoT network. Moreover, we investigate the impact of this interference on the average AoI of the *segmented* packets considering both preemptive and non-preemptive approaches.

From the perspective of queueing theory, the AoI of transmitted packets has been derived considering different queueing disciplines, such as First Come First Serve (FCFS) or Last Come First Serve (LCFS). Based on the FCFS approach, M/M/1, and M/M/D queueing systems, a closed-form expression for AoI was derived in [9] by considering a violation

The authors would like to acknowledge the support provided by the Deanship of Research Oversight and Coordination (DROC) at King Fahd University of Petroleum & Minerals (KFUPM) for funding under the Interdisciplinary Research Center for Communication Systems and Sensing through project No. INCS2201.

probability that AoI exceeds a specific age constraint. LCFS M/M/1/1 preemptive queue is considered in [10] to determine the correlation between the service time and the interarrival time of the new updates to compute the AoI. In [11], the authors investigated different service time distributions to minimize AoI where they considered two policies: LCFS preemptive policy and LCFS non-preemptive policy. Under the assumption of an exponential service time, the LCFS preemptive policy was shown to minimize the AoI. Then by involving New Better than Used (NBU) distributions for the service time, the authors proved that the LCFS non-preemptive policy has a small gap from the optimal AoI value, which is independent of the system parameters.

Our main contributions are listed as follows.

1) We analyze the average AoI in large-scale IoT networks, based on a spatiotemporal model for the SD pairs, under preemptive and non-preemptive transmission schemes.
2) We study the effect of packet segmentation on the average AoI for both schemes.
3) We compare both schemes for different transmission classes, packet sizes, and the number of segments.

Our results show that none of the two transmission schemes will always outperform the other. Based on the system parameters, either scheme can result in a lower AoI. Moreover, our results show that packet segmentation can be beneficial in reducing the AoI, especially for large packet sizes.

II. System Model

A. Network Model

A target IoT link is assumed to exist within a heterogeneous Poisson field (HPF) of interferers. The distance between the transmitter and receiver of the target IoT link is assumed to be D meters. The HPF represents the interference from other coexisting IoT devices, which share the same spectrum and are spatially distributed according to a PPP Ψ in $\mathbb{R}^2$ with intensity λ. To account for the diverse types of the IoT devices, the HPF consists of v different network types, where $v = \{1, 2, 3, \cdots, V\}$. Assuming that the type of the IoT device is independent of its spatial location, Ψ can be divided into V independent PPPs, which are denoted as Ψ_v with intensities $\lambda_v = f_v(v)\lambda$, where $f_v(v)$ is the probability of being of type v. The IoT devices of different types differ in their transmission powers w_v and activity factors k_v.

We consider a time-slotted system with a fixed time-slot duration of T_s seconds. Within each time slot, the transmitter of the target IoT link randomly generates an update packet of size $\mathcal{L}$ bits with probability a. The parameters $\mathcal{L}$ and a determine, respectively, the update quality and temporal resolution [12]. For reliable transmissions [13], large packets can be divided into n smaller segments with equal sizes of length $\mathcal{L}/n$ bits. The segments are sequentially transmitted, one per time slot, to the target receiver. The transmitting power is w_t watts, and the transmission rate is

$$\mathcal{R}_n = \frac{\mathcal{L}}{n \times T_s} = \zeta W \log_2(1 + \theta_n), \tag{1}$$

where $0 < \zeta \leq 1$ captures the gap between practical transmission rates compared to Shannon's capacity, W is the channel bandwidth, and θ_n is the minimum required signal-to-interference-ratio (SIR) threshold. That is, a segment $i \in \{1, 2, \cdots, n\}$ within the packet is successfully decoded at the target receiver if the SIR exceeds the threshold θ_n.

A Rayleigh fading environment is considered, where $h \sim \mathcal{CN}(0, 1)$ is the normalized baseband channel gain. Due to channel fading and interference, transmissions of the target link may fail. Let $P_n = \mathbb{P}\{(SIR > \theta_n)|\Psi\}$ denote the success probability to transmit one segment with rate R_n. The SIR at the target receiver is expressed as:

$$SIR = \frac{w_t h_0 D_0^{-\eta}}{\sum_{v=1}^{V} \sum_{D_u \in \Psi_v} \mathbb{I}_u w_v h_u D_u^{-\eta}} \tag{2}$$

where h_0 channel gain of the intended transmitter, h_u is the channel gain from the u-th interfering IoT device, η is the path-loss exponent, and $\mathbb{I}_u$ is an indicator factor that accounts for its activity. Assuming an arbitrary but fixed realization of Ψ and a target link rate of $\mathcal{R}_n$, the segment successful transmission probability can be expressed as

$$P_n(\Psi) = \mathbb{P}\left(\frac{w_t h_0 D_0^{-\eta}}{\sum_{v=1}^{V} \sum_{D_u \in \Psi_v} \mathbb{I}_u w_v h_u D_u^{-\eta}} > \theta_n | \Psi \right). \tag{3}$$

It is worth noting that the locations of the interfering IoT devices are fixed to account for the much faster variations of the channel gains and transmission activities when compared to the variations of the IoT devices locations.

B. Preemptive/Non-preemptive Transmission Models

We consider a simple IoT transmitter of the target link with a one-packet queue size. The IoT transmitter can follow either a preemptive or a non-preemptive transmission scheme to deliver the packet to the target receiver. In the preemptive scheme, the IoT transmitter serves the most recent update. If the queue is non-empty, a newly generated update in the preemptive scheme overwrites the packet in service. In the non-preemptive scheme, the transmitter is obligated to finish the transmission of the packet in service before accepting a new packet. This means that if the queue is non-empty, a newly generated update in the non-preemptive scheme is discarded.

At first glance, it may appear that the AoI of the preemptive scheme will always outperform its non-preemptive counterpart because the former always serves the most recent update. However, this is not necessarily true for packet segmentation. Recall that large packets are divided into n smaller segments that need at least n time slots to be successfully delivered. This implies that the preemptive scheme wastes any partial delivery (i.e., any $m < n$ delivered segments) of a packet upon a new packet arrival. On the other hand, the non-preemptive scheme consistently transmits all segments of each packet in service at the expense of discarding new updates.

Pictorial illustrations of the two schemes for $n = 5$ are given in Figs. 1 and 2. Fig. 1 shows the AoI of the non-preemptive scheme, where new updates (represented by green

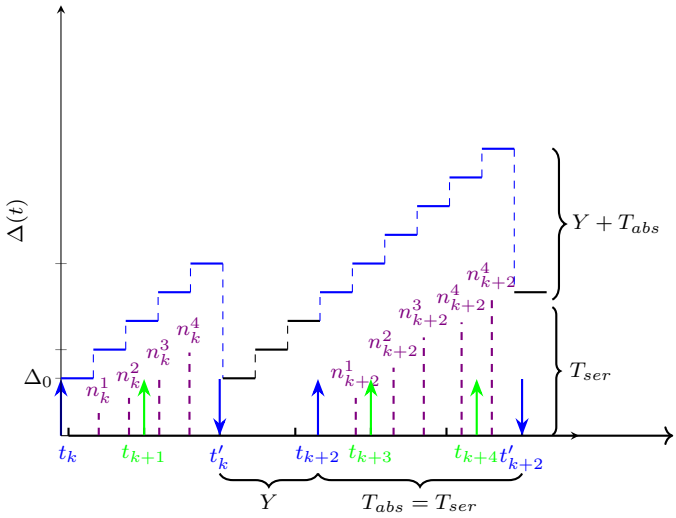

Fig. 1: AoI evolution for a five-segment packet transmission under the non-preemptive approach. Upwards and downwards blue arrows are generation and reception of the transmitted packet, while green upwards arrows show ignoring of the new packets when a packet is being served.

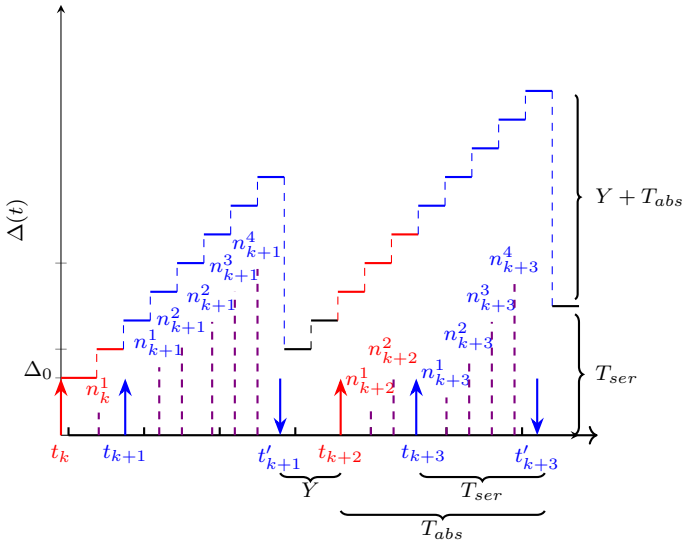

Fig. 2: AoI evolution for a five-segment packet transmission under the preemptive approach. Upwards and downwards red and blue arrows denote the generation and reception of the transmitted packet, whereas two consecutive upwards arrows indicate new packets preempting the in-service packets.

arrows) are dropped until the successful transmission of all segments of the currently serviced update (represented by a blue color). For example, in Fig. 1, Packet $k+1$ (represented as a green arrow) is generated during the service time of Packet k (the blue portion of the curve), and hence it is dropped. After the successful delivery of Packet k at t'_k, The transmitter can then accept a new update for service, which is generated in the figure at t_{k+2}. The lack portion of the curve represents the waiting time until a new packet is generated at the transmitter. The number of time slots required to transmit a packet is random and depends on the probability of successful transmission of the segments. Fig. 2 shows the AoI of the preemptive scheme, where new updates (blue portions of the curve) overwrite the packets being in service (red portions of the curve). Hence, a successful transmission for any packet k requires successfully transmitting all of its segments before the arrival of a new packet.

The AoI, denoted as $\Delta(t)$, is the elapsed time since the generation of the last successfully received packet. Therefore, assuming that the last successfully delivered packet is Packet k, then $\Delta(t) = t - t_k$, where t_k is the generation time of Packet k. As shown in Figs. 1 and 2, starting from an initial AoI $\Delta(0) = \Delta_0$, the discretized AoI at the receiver increases with time in a staircase fashion and drops upon the reception of a new packet (at instants t'_k and t'_{k+2} in Fig. 1, and instants t'_{k+1} and t'_{k+3} in Fig. 2).

III. Age of Information (AoI) Analysis

For a given realization of Ψ, the transmission success probability (TSP) is given by

$$P_n(\Psi) = \prod_{v=1}^{V} \prod_{D_u \in \Psi_v} \left(\frac{k_v}{1 + \theta_n \frac{w_v D_0^{\eta}}{w_t D_u^{\eta}}} + (1 - k_v) \right), \quad (4)$$

where (4) follows from averaging (3) over the channel gains and devices activities [13]. Since there is no prior knowledge about the specific realization of the interfering IoT network Ψ, we utilize the meta distribution to find the likelihood that the target link operates at a given success probability [14]. The meta distribution of the TSP is formally defined as

$$\bar{F}(\theta_n, \gamma) = \mathbb{P}\{\mathbb{P}(SIR > \theta_n | \Psi) > \gamma\} = \mathbb{P}(P_n(\Psi) > \gamma), \quad (5)$$

where $\bar{F}(\theta_n, \gamma)$ quantifies the percentile of the HPF realizations in which the target link operating at rate $\mathcal{R}_n$ will achieve a TSP greater than γ. Following [13] and [14], for a certain rate $\mathcal{R}_n$, a tight approximation for the meta distribution in (5) can be obtained as stated in the following proposition.

Proposition 1. *For a given θ_n, the percentile of the HPF realizations where the target link achieves a TSP greater than γ is captured by the following:*

$$\bar{F}(\theta_n, \gamma) = 1 - \mathcal{I}_{\gamma} \left(\frac{\mu_n(\mu_n - \nu_n)}{\nu_n - \mu_n^2}, \frac{(1 - \mu_n)(\mu_n - \nu_n)}{\nu_n - \mu_n^2} \right), \quad (6)$$

where $\mathcal{I}_{\gamma}(a, b)$ is the regularized incomplete beta function, μ_n is the first moment and ν_n is the second moment of the TSP for rate $\mathcal{R}_n$ across different realizations of the HPF. Let $\Lambda = \frac{-2(\pi D_0)^2}{\eta \sin(2\pi/\eta)}$, then μ_n and ν_n are given by

$$\mu_n = \exp\left(-\Lambda \theta_n^{\frac{2}{\eta}} \sum_{v=1}^{V} \left(\frac{w_v}{w_t} \right)^{\frac{2}{\eta}} k_v \lambda_v \right), \quad (7)$$

$$\nu_n = \exp\left(-\Lambda \theta_n^{\frac{2}{\eta}} \sum_{v=1}^{V} \left(\frac{w_v}{w_t} \right)^{\frac{2}{\eta}} k_v \lambda_v \left(2 - \left(1 - \frac{2}{\eta} \right) k_v \right) \right), \quad (8)$$

Proof. The proof can be obtained by following the same steps as in [13]. □

To account for the impact of the HPF realization on the target link, $\bar{F}(\theta_n, \gamma)$ in (6) is discretized to C equiprobable TSP classes for each rate R_n. Let $w_0 = 0$ and $w_C = 1$, and choose $\{w_1, w_2, w_3, \cdots, w_{C-1}\}$ such that the TSP of class i satisfies the following equation for $i = 1, 2, \cdots, C-1$

$$\bar{F}(\theta_n, w_i) - \bar{F}(\theta_n, w_{i-1}) = \frac{1}{C} \tag{9}$$

Hence, TSPs within the range $[w_c, w_{c+1}]$ are approximated by the median value $p_{n,c}$ which can be calculated from

$$\bar{F}(\theta_n, w_c) - \bar{F}(\theta_n, p_{n,c}) = \frac{1}{2C}. \tag{10}$$

To track the AoI of the target link, we construct a discrete-time absorbing Markov chain (DT-AMC) for each (n, c) pair. For a given packet segmentation n, the DT-AMC tracks the successful transmission of the segments, where the HFP interference impact is considered by using $p_{n,c}$ obtained from (10) as the segment departure probability. The absorption state of the DT-AMC implies that all segments are successfully transmitted, and hence, the packet is usefully delivered to its destination. To have a unified formulation of the preemptive and non-preemptive transmission schemes, we introduce the factor $\alpha \in \{0, 1\}$, such that $\alpha = 0$ captures the non-preemptive scheme and $\alpha = 1$ captures the preemptive scheme. The unified DT-AMC is shown in Fig 3 and has the transition matrix given by

$$T_{n,c} = \left[\begin{array}{c:c} Q_{n,c} & H_{n,c} \\ \hdashline 0 & 1 \end{array}\right] = \left[\begin{array}{ccccccccc:c} \alpha a + q_1 & q_2 & 0 & 0 & 0 & 0 & \cdots & 0 & 0 \\ \alpha a & q_1 & q_2 & 0 & 0 & 0 & \cdots & 0 & 0 \\ \alpha a & 0 & q_1 & q_2 & 0 & 0 & \cdots & 0 & 0 \\ \alpha a & 0 & 0 & q_1 & q_2 & 0 & \cdots & 0 & \vdots \\ \vdots & 0 & \ddots & \ddots & \ddots & \ddots & \ddots & \vdots & 0 \\ \alpha a & 0 & \cdots & 0 & 0 & 0 & 0 & q_1 & q_2 \\ \hdashline 0 & 0 & 0 & 0 & 0 & 0 & 0 & 0 & 1 \end{array}\right], \tag{11}$$

where $q_1 = \bar{p}_{n,c}(1 - \alpha a)$ and $q_2 = p_{n,c}(1 - \alpha a)$. In (11), Q is $[n \times n]$ sub-stochastic matrix that tracks the transmissions of the n segments that belong to a given packet and H is $(n \times 1)$ vector that tracks the transition of the absorbing state, which implies the successful delivery of the last segment. Since we always start from the first segment, upon packet arrival, the initialization vector for the DT-AMC is $\beta = [1, 0, 0, \cdots, , 0]$ of size $(1 \times n)$. It is worth noting that the αa factor in the first column accounts for the packet preemption, in which the transmissions of old segments are wasted and the DT-AMC is restarted for the new packet.

In order to calculate the average AoI, we need to define three quantities; namely, the average time to absorption T^n_{abs}, the average service time T^n_{ser}, and the average inter-arrival time Y. The time to absorption for the DT-AMC in (11) tracks the time taken from the first packet generation time, after the successful delivery of a previous packet, to the next successful packet delivery to the target receiver for rate R_n. The average number of time slots required before absorption can be obtained as

$$M^n_{abs} = \beta (I - Q_{n,c})^{-2} H_{n,c} \tag{12}$$

where I is an identity matrix with $(n \times n)$ dimensions. Assuming that the time slot duration is normalized to unity, the average time to absorption is $T^n_{abs} = M^n_{abs}$.

Let $M^n_{ser,k}$ denote the number of time slots required to deliver all n segments of packet k, i.e., the number of time slots required to service Packet k. Assuming unity time slot, we have $T^n_{ser,k} = M^n_{ser,k=t'_k - t_k}$. It is straightforward to show that $M^n_{ser,k}$ has the following distribution:

$$\begin{aligned} &\mathbb{P}\{M^n_{ser,k}, n \text{ segments are delivered}\} \\ &= \binom{M^n_{ser,k} - 1}{n - 1} P^n_n (1 - P_n)^{M^n_{ser,k} - n} (1 - \alpha a)^{M^n_{ser,k} - 1}, \end{aligned} \tag{13}$$

and

$$\begin{aligned} &\mathbb{P}\{M^n_{ser,k}/n \text{ segments are delivered}\} \\ &= \frac{\mathbb{P}\{M^n_{ser,k}, n \text{ segments are delivered}\}}{\sum_{i=n}^{\infty} \mathbb{P}\{i, n \text{ segments are delivered}\}}. \end{aligned} \tag{14}$$

Using the distribution in (14), the average service time of a packet T^n_{ser} can be calculated. Note that in the non-preemptive case, we have $T^n_{ser} = T^n_{abs}$.

Now, define Y as the inter-arrival time between the successful delivery of one packet at the receiver and the generation of the next packet at the transmitter. The distribution of Y can be written as $\mathbb{P}(Y = X) = a(1 - a)^{X-1}$, from which we can calculate the average of Y.

Given the previous three definitions of T^n_{ab}, T^n_{ser}, and Y, the average AoI can be calculated as:

$$\text{AoI} = T^n_{ser} + \frac{T^n_{abs} + \mathbb{E}(Y)}{2}. \tag{15}$$

IV. Numerical Results

We use Monte Carlo simulation to construct $\bar{F}_{Sim}(\theta_n, \gamma)$ across 1000 different HPF realizations via 10^4 time iterations within a simulation area of radius 1200 meters for $C = 35$ classes. Unless otherwise stated, the parameters of HPF are set as $\lambda = 0.001$ device/km^2 that are divided into $V = 3$ different networks, with uniform distribution $f_v(v) = 1/3$ where $v \in \{1, 2, 3\}$ with transmit power and activity factors $w \in \{10, 7, 5\}$ mWatt and $k \in \{0.1, 0.3, 0.5\}$, respectively. The arrival rate and the link parameters are set as $a = 0.1$, $W = 100$ KHZ, $T_s = 1$ ms, $\zeta = 0.8$, $\eta = 4$, $D_0 = 20$ meters, and $N = 5$ rates.

Fig. 4 shows $\bar{F}(\theta_n, \gamma)$ for each transmission rate. For the analysis part, the meta distribution in (6) is divided into C equiprobable TSP classes for different HPF realizations; $p_{n,c}$ is the median value within the corresponding TSP range. Thereafter, $p_{n,c}$ is used to construct the queuing model to find the time to absorption and AoI as well. Analysis and simulation results of each TSP meta distribution for a packet size of

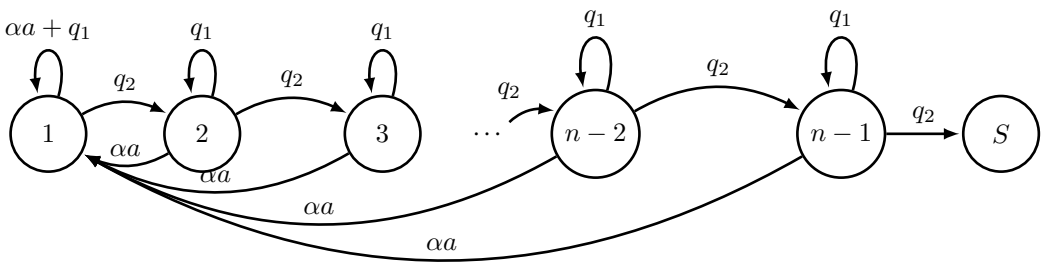

Fig. 3: Absorbing Markov chain for transmission of one packet which is segmented into n segments.

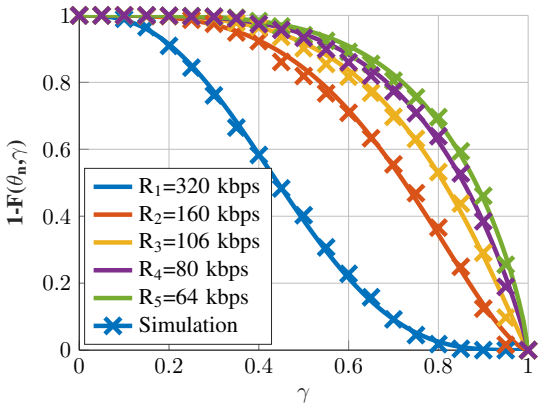

Fig. 4: TSP meta distribution for different values of $\mathcal{R}_n$.

$L = 40$ Bytes, hence $R_n = 320/n$ where $n \in \{1, 2, 3, 4, 5\}$ segments, are shown in Fig. 4; this figure clearly shows the matching results for the different transmission rates.

To compare the preemptive and non-preemptive transmission schemes, we consider three different TSP classes, where the first class is a highly congested class, the second one has medium congestion, and the last one has the lowest congestion. We assume an arrival rate of $a = 0.1$ and different packet sizes of 40, 60, and 120 bytes. We assume that the number of segments, n, is such that $n \in \{1, 2, 3, 4, 5\}$ segments. Accordingly, the packet transmission rate satisfies $\mathcal{R}_n = \dfrac{\mathcal{L}}{n \times T_s}$ based on the number of segments.

In Fig. 5, we can see that the average AoI of the un-segmented packet case is lower than the AoI in the case of segmented packets, for both the preemptive scheme and the non-preemptive schemes, for all classes with the smallest packet size (40 Bytes). While in Figs. 6 and 7, which is the case of larger packets, packet segmentation can result in reducing the average AoI. Fig. 6 shows that for 60 Bytes packet size, segmentation of the packets into two segments ($n = 2$) achieves the lowest average AoI for the highest congested class, while the un-segmented case is more suitable for both the medium and low congestion classes. However, in Fig. 7, for a larger packet size (120 Bytes), packet segmentation can reduce the average AoI from infinity in the case of unsegmented packets to finite values for the segmented cases for all categories of transmission classes. As we can see for the highest and medium congested classes (class 1 and 2, respectively), the smallest average AoI can be achieved when the packets are divided into three segments ($n = 3$). While for the lowest congested class (class 3), the average AoI is reduced when the number of segments is $n = 2$ and $n = 3$ for preemptive and non-preemptive schemes, respectively. Also, we can see very small performance gaps between the two transmission schemes for medium and low congestion classes regardless of the packet size. In conclusion, our results show that none of the two schemes will always outperform the other. The superiority of one scheme depends on the system parameters such as the packet size, number of segments, channel quality, etc.

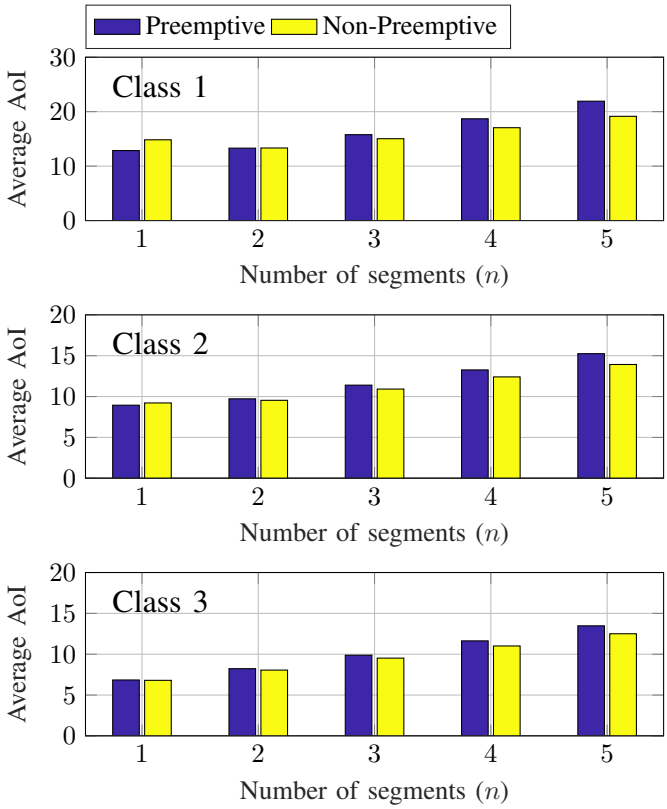

Fig. 5: Average AoI under non-preemptive and preemptive schemes for a 40-Byte packets and different segmentation.

V. Conclusion

In this paper, we utilized a spatiotemporal mathematical model to characterize the AoI of a target IoT link existing

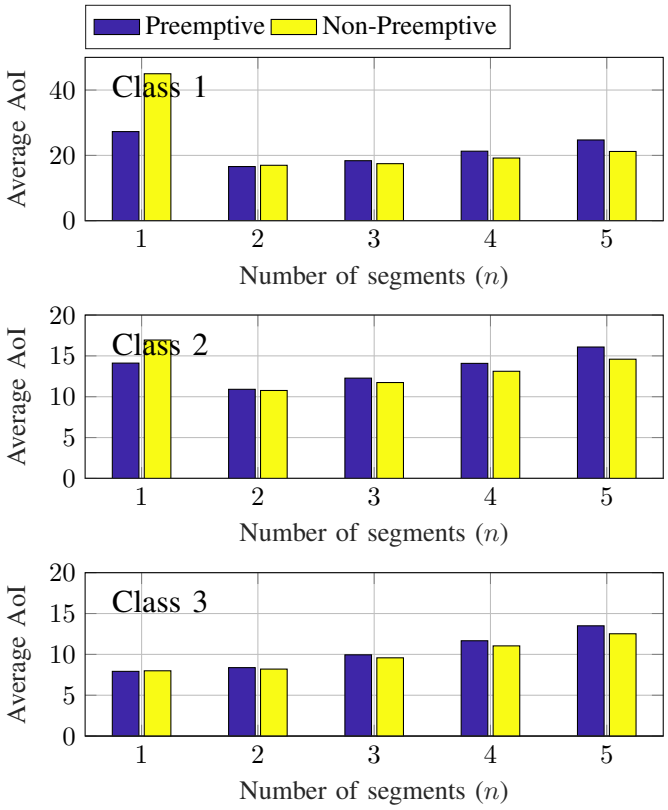

Fig. 6: Average AoI under non-preemptive and preemptive schemes for a 60-Byte packets and different segmentation.

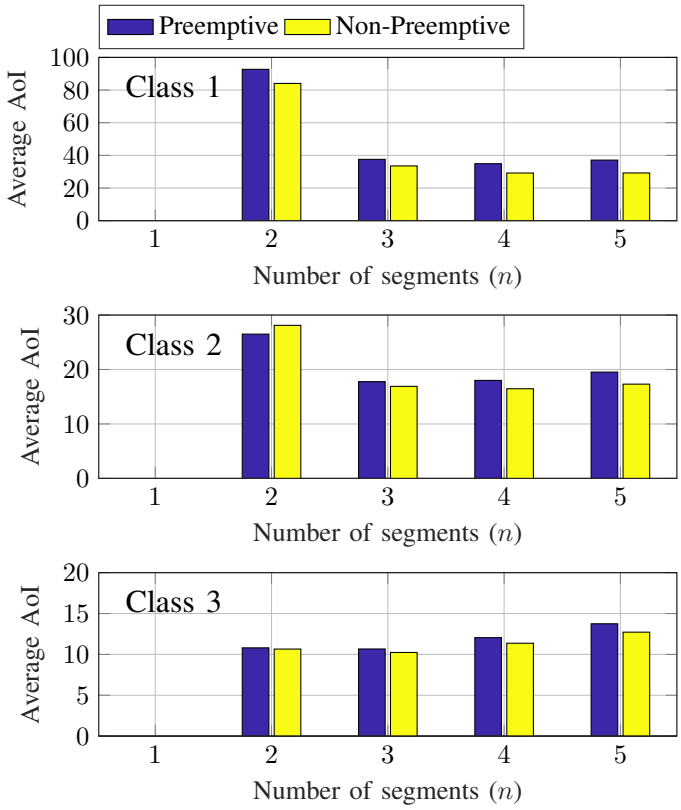

Fig. 7: Average AoI under non-preemptive and preemptive schemes for a 120-Byte packets and different segmentation (empty bars represent infinite average AoI).

in a large-scale IoT network. The network is modeled via a heterogeneous Poisson field (HPF) of interferes. Preemptive and non-preemptive transmission schemes are considered, where we analytically characterize the average AoI via an absorbing Markov chain. Moreover, the AoI is investigated for different congestion levels in the network as well as different packet sizes and different numbers of segments. In contrast to the single segment case, where the preemptive scheme always outperforms the non-preemptive scheme, our results show that the superiority of one transmission scheme depends on the system parameters. For large packets where segmentation is necessary, the non-preemptive scheme may outperform the preemptive scheme. That is, the persistence to deliver the remaining segments of an old packet may be preferable than restarting the segments transmission of a new packet. For a given packet size and channel quality, minimizing the average AoI requires careful selection of the number of packet segments and the transmission scheme.

REFERENCES

[1] S. K. Kaul, R. D. Yates, and M. Gruteser, "Real-time status: How often should one update?" *2012 Proceedings IEEE INFOCOM*, pp. 2731–2735, 2012.

[2] A. Kosta, N. Pappas, and V. Angelakis, *Age of Information: A New Concept, Metric, and Tool*, 2017, vol. 12.

[3] B. Buyukates, A. Soysal, and S. Ulukus, "Age of information scaling in large networks," in *ICC 2019 - 2019 IEEE International Conference on Communications (ICC)*, 2019, pp. 1–6.

[4] Y. Sun, E. Uysal-Biyikoglu, R. D. Yates, C. E. Koksal, and N. B. Shroff, "Update or wait: How to keep your data fresh," *IEEE Transactions on Information Theory*, vol. 63, no. 11, pp. 7492–7508, 2017.

[5] R. Talak, S. Karaman, and E. Modiano, "Optimizing age of information in wireless networks with perfect channel state information," in *2018 16th International Symposium on Modeling and Optimization in Mobile, Ad Hoc, and Wireless Networks (WiOpt)*, 2018, pp. 1–8.

[6] M. A. Abd-Elmagid and H. S. Dhillon, "Average peak age-of-information minimization in uav-assisted iot networks," *IEEE Transactions on Vehicular Technology*, vol. 68, no. 2, pp. 2003–2008, 2019.

[7] M. Emara, H. ElSawy, and G. Bauch, "A spatiotemporal model for peak aoi in uplink iot networks: Time versus event-triggered traffic," *IEEE Internet of Things Journal*, vol. 7, no. 8, pp. 6762–6777, 2020.

[8] P. D. Mankar, M. A. Abd-Elmagid, and H. S. Dhillon, "Spatial distribution of the mean peak age of information in wireless networks," *IEEE Transactions on Wireless Communications*, vol. 20, no. 7, pp. 4465–4479, 2021.

[9] L. Hu, Z. Chen, Y. Dong, Y. Jia, L. Liang, and M. Wang, "Status update in iot networks: Age-of-information violation probability and optimal update rate," *IEEE Internet of Things Journal*, vol. 8, no. 14, pp. 11 329–11 344, 2021.

[10] R. D. Yates, "Age of information in a network of preemptive servers," in *IEEE INFOCOM 2018 - IEEE Conference on Computer Communications Workshops (INFOCOM WKSHPS)*, 2018, pp. 118–123.

[11] A. M. Bedewy, Y. Sun, and N. B. Shroff, "Minimizing the age of information through queues," *IEEE Transactions on Information Theory*, vol. 65, no. 8, pp. 5215–5232, 2019.

[12] Y. Nabil, H. ElSawy, S. Al-Dharrab, H. Mostafa, and H. Attia, "Data aggregation in regular large-scale iot networks: Granularity, reliability, and delay tradeoffs," *IEEE Internet of Things Journal*, pp. 1–1, 2022.

[13] H. ElSawy, "Rate adaptation and latency in heterogeneous iot networks," *IEEE Communications Letters*, vol. 25, no. 2, pp. 660–664, 2021.

[14] M. Haenggi, "The meta distribution of the sir in poisson bipolar and cellular networks," *IEEE Transactions on Wireless Communications*, vol. 15, no. 4, pp. 2577–2589, 2016.